Performance of cryogenic oxygen production unit with exhaust gas bleed for sewage sludge gasification and different oxygen purities

MAJA KASZUBA[*]
PAWEŁ ZIÓŁKOWSKI
DARIUSZ MIKIELEWICZ

Gdańsk University of Technology, Narutowicza 11/12, 80-233 Gdańsk, Poland

Abstract The paper presents a thermodynamic analysis of the integration of a cryogenic air separation unit into a negative CO_2 emission gas power plant. The power cycle utilizes sewage sludge as fuel so this system fits into the innovative idea of bioenergy with carbon capture and storage. A cryogenic air separation unit integrated with the power plant was simulated in professional plant engineering and thermodynamic process analysis software. Two cases of the thermodynamic cycle have been studied, namely with the exhaust bleed for fuel treatment and without it. The results of calculations indicate that the net efficiencies of the negative CO_2 emission gas power plant reach 27.05% (combustion in 95.0% pure oxygen) and 24.57% (combustion in 99.5% pure oxygen) with the bleed. The efficiencies of the cycle without the bleed are 29.26% and 27.0% for combustion in 95.0% pure oxygen and 99.5% pure oxygen, respectively. For the mentioned cycle, the calculated energy penalty of oxygen production was 0.235 MWh/kgO$_2$ for the lower purity value. However, for higher purity namely 99.5%, the energy penalty of oxygen production for the thermodynamic cycle including the bleed and excluding the bleed was indicated 0.346 and 0.347 MWh/kgO$_2$, respectively. Additionally, the analysis of the oxygen purity impact on the carbon dioxide purity at the end of the carbon capture and storage installation shows that for the case with the bleed, CO_2 purities are 93.8% and 97.6%, and excluding the bleed they are 93.8% and 97.8%, for the mentioned oxygen purities respectively. Insertion of the cryogenic oxygen production in-

---

[*]Corresponding Author. Email: maja.kaszuba@pg.edu.pl

stallation is required as the considered gas power plant uses oxy-combustion to facilitate carbon capture and storage method.

Nomenclature

c	–	velocity, m/s
eCO_2	–	emissivity of CO_2, $kgCO_2$/MWh
e_{pen}	–	energy penalty, MWh/kgO_2
g	–	gravitational acceleration, m/s^2
LHV	–	lower heating value, MJ/kg
$\dot{m}$	–	mass flow rate, kg/s
N_{ASU}	–	power for air separation needs, kW
$N_{C_{\mathrm{CCS}}}$	–	power for CCS compressors needs, kW
N_{CP}	–	total power for own needs, kW
$N_{C_{\mathrm{fuel}}}$	–	power for fuel compressor needs, kW
$N_{C_{\mathrm{O2}}}$	–	power for oxygen compressor needs, kW
$N_{P_{\mathrm{H2O}}}$	–	power for water pump needs, kW
$N_{P_{\mathrm{SEC}}}$	–	power for SEC pump needs, kW
N_t	–	combined turbines power, kW
R	–	factor describing energy source as renewable
t	–	temperature, °C
$\dot{Q}_{CC}$	–	chemical rate of combustion, kW
u	–	internal energy, kJ/kg
XCO_2	–	volume fraction of carbon dioxide, %
z	–	height, m

Greek symbols

η_{cum}	–	cumulative efficiency, %
η_{g}	–	gross efficiency of the cycle, %
η_{net}	–	net efficiency of the cycle, %
η_{R_H}	–	gasifier efficiency, %
ρ	–	density, kg/m^3

Acronyms

ASU	–	air separation unit
BCCS	–	bioenergy with carbon capture and storage
CCS	–	carbon capture and storage
GS	–	gas scrubber
GT	–	gas turbine
HE	–	heat exchanger
nCO2PP	–	negative CO_2 emission gas power plant
PC	–	pre-cooler
SEC	–	spray ejector condenser
WCC	–	wet combustion chamber

1 Introduction

It is estimated that the production of electric power contributes to the generation of approximately 25.0% of CO_2 in the atmosphere [1, 2]. Over the years, several ways for reducing CO_2 from the atmosphere were introduced. These solutions can be divided generally into oxy-combustion, post-combustion, and pre-combustion [3]. In post-combustion technology, CO_2 is captured after the combustion process from flue gases. It can be done in several ways including sorption technologies, membrane separation, and cryogenic distillation [3–5]. A very crucial advantage of the post-combustion method is that it can be introduced to existing power plants, and a disadvantage is that CO_2 concentration in exhaust gases is very low and the exhaust pressure is near the atmospheric pressure [3]. According to the literature, the most mature way to separate CO_2 from the rest of the flue gas is absorption and its energy requirement contributes to $13.0-15.0\%$ of the power plant efficiency [3].

The pre-combustion technology assumes carbon removal from the fuel before the combustion process. This process consists of two parts. In the first one, the mixture of H_2 and CO is obtained from gas reforming, then in the second part, CO is altered into CO_2 and separated from H_2. In the end, only H_2 is combusted. The power cycles coupled with pre-combustion technology are called integrated gasification combined cycles (IGCC) [3].

Oxy-fuel is the third carbon capture and storage method, next to post-combustion and pre-combustion. It is probably the most promising solution for power plants that require carbon capture and storage (CCS) technology. In particular, in the case of the connection between increasing global electricity production and growing CO_2 concentration in the atmosphere. Future power plants will need to feature the CCS installations [6, 7], due to the need of stopping and avoiding an increase in CO_2 concentration in the atmosphere. A typical power plant worked with oxy-combustion technology would require 20 tons of O_2 for each megawatt per day [8–10]. Oxygen can be produced in several ways. The most popular are cryogenic air distillation, followed by pressure swing adsorption, oxygen transport membranes, chemical looping air separation, and electrolysis of water [11]. For the combustion process, low-purity oxygen in the range of $85.0-98.0\%$ is supposed to be the most appropriate. It is connected with high energy consumption while producing oxygen purer than 95.0% with the cryogenic air distillation method. This technology will be taken into consideration

in this work and will be connected with the negative CO_2 emission gas power plant.

Cryogenic air distillation is the most developed technology in oxygen production [11]. Its biggest disadvantage is that oxygen production is very energy-consuming. On the other hand, cryogenic separation is the only technology that can provide huge capacities of produced oxygen. Additionally, other air gases which are also industrial gases are possible to be obtained [10]. The minimum thermodynamic work needed to produce oxygen is 0.051 MWh/kgO_2 but in real cryogenic installations, it is approximately four times greater [12].

Conventional cryogenic double-column air separation unit consists of an air compressor considered the most energy-consuming device in the installation [9], two thermally-coupled rectification columns, and heat exchangers. In the first step, the air is compressed usually to $5.4-6.0$ bar [13,14]. Next, it is cooled in a heat exchanger called a pre-cooler, then separated into two streams. One of the streams is introduced into the high-pressure column and the second into the low-pressure column. At the top of the high-pressure column, nitrogen is obtained at a pressure of 6.0 bar. At the bottom of mentioned column oxygen-enriched liquid is obtained. Obtained nitrogen is condensing because of boiling oxygen in the reboiler, which connects two columns. Both product streams obtained at the high-pressure column are depressurized and sent to the low-pressure column. In this column, gaseous nitrogen is obtained at the top of the tower, and liquid oxygen at the bottom [13,14]. The distillation process is based on differences in boiling points of air components at specified pressures [15].

The paper presents the results of an integration of a cryogenic air separation unit (ASU) into a negative CO_2 emission gas power plant (nCO2PP) and the impact of the oxygen production installation on the power cycle. For this thermodynamic cycle, other oxygen production methods might be considered such as membrane or sorption techniques. Some of these technologies were compared with cryogenic air distillation in other works [16–18]. However, when it comes to large scale power plants with a capacity of hundreds of megawatts, cryogenic air separation is the only appropriate solution [19], because only this method is able to produce huge amounts of oxygen up to 150 000 m^3/h [20]. Moreover, it is the most developed way to produce oxygen from the air. Due to its maturity, low-temperature technology was chosen.
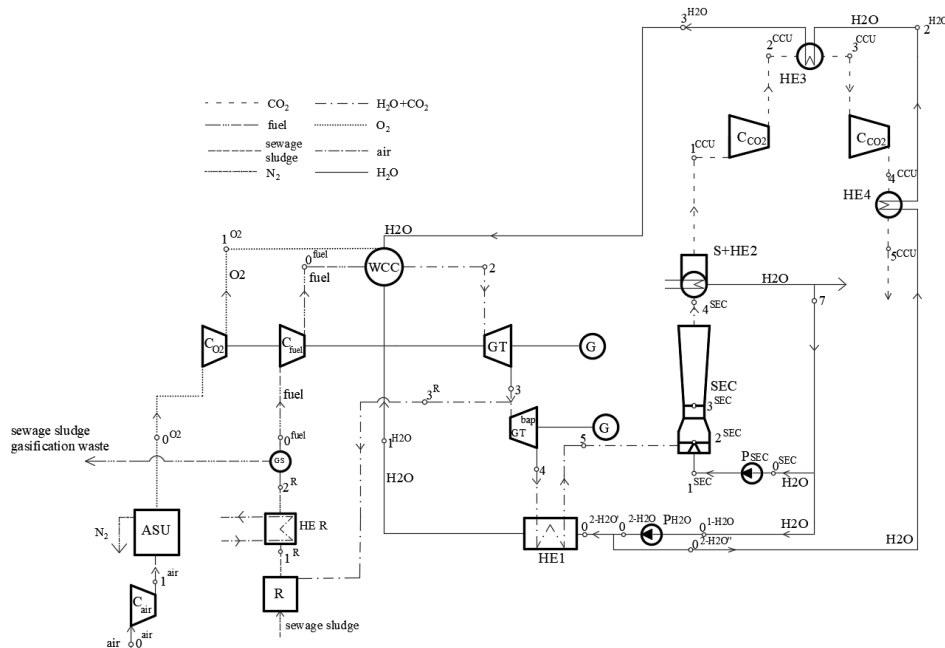
2   Negative CO₂ emission gas power plant integrated with cryogenic air separation unit

Over the years, several configurations of power cycles with oxy-fuel technology have been proposed, with either gas or coal fuels. The common entity for all these cycles was the oxygen as an oxidizer and then flue gases composed of steam and carbon dioxide. Part of the solutions recovers the carbon dioxide from exhaust gases, recirculates it to the combustion chamber, and uses it as a working medium in the cycle [21–23]. Most oxy-fuel cycles are integrated by a heat recovery steam generator with the Rankine cycle to avoid huge heat losses [24].

The scrutinised nCO2PP cycle is a gas-steam turbine cycle integrated with a CCS installation and a cryogenic ASU. The power plant is fuelled with syngas from the gasification process of sewage sludge. The combustion process takes place in the atmosphere of pure oxygen and the combustion chamber is cooled by water injection. The considered thermodynamic cycle has been studied before in other works [25], but its integration with an ASU has not been taken into consideration.

The diagram of nCO2PP is presented in Fig. 1. The system is equipped with two compressors. The first one forces the flow of oxidant (C_{O2}), whereas the second one is for the fuel transport (C_{fuel}). The cycle also consists of the high-pressure gas turbine (GT), low-pressure gas turbine (GT^{bap}), wet combustion chamber (WCC), and generator (G). The main heat exchanger (HE1) heats the water supplied to the WCC with exhaust gases. The spray-ejector condenser (SEC) is a novel device for the exhaust gas condensation process. A CCS installation consists of two compressors (C_{CO2}), two heat exchangers (HE3, HE4), and a heat exchanger connected with a water separator (S+HE2). The water pump (P_{H2O}) increases the pressure of water, which is supplied to the WCC. Between two expanders is an exhaust bleed for the needs of the gasification process. Sewage sludge gasification takes place in the gasifier (R). A heat exchanger (HE R) and a gas scrubber (GS) are also on the fuel way to the combustion chamber.

According to the calculations, exhaust gases contain mostly steam. Indeed, oxygen and fuel are supplied by compressors, as they are present in gas turbines, but there is much more water injected into the combustion chamber by the pump. This amount of water exceeds the fuel and oxidizer streams. An additional characteristic of steam cycles is the presence of a condensation process, which is also characteristic to the considered nCO2PP cycle.

Figure 1: Diagram of negative CO_2 emission gas power plant.

The beginning of the process in the cycle can be established when fuel and oxygen compressors (C_{fuel}, C_{O2}) start transporting fluids to the combustion chamber (WCC). In the combustion chamber fuel, oxygen, and injected water, due to high temperature processes, create a mixture of carbon dioxide and water. Water injection is necessary, because of high temperatures, which are the effect of the oxy-combustion process. Additionally, the extra mass flow of water contributes to the increase of the turbines power, which is dependent on the mass flow. After the combustion process, expansion in two turbines (GT, GT^{bap}) takes place. Afterwards, exhaust gases are heating water, which is transported by the pump (P_{H2O}) to the combustion chamber, through the heat exchanger (HE1). The spray-ejector condenser (SEC) intakes the flue gases from the heat exchanger (HE1). Provided is also water, which is a motive fluid in the SEC with the pump (P_{SEC}). The presence of motive water, which breaks up into droplets, and the mixture of steam and carbon dioxide enables the condensation process to take place. The mixture of water and carbon dioxide leaving the SEC goes to the separator connected to the heat exchanger (S+HE2). Water is isolated and directed to pumps (PSEC, PH2O) in the separator. Subsequently, it

is used as the motive fluid in SEC or as a cooling fluid in the combustion chamber (WCC). The carbon dioxide is directed to the compressor (C_{CO2}) and the heat exchanger (HE3).

The oxygen, which is an oxidant in the combustion process in the WCC, is supplied from the cryogenic air separation unit. Air separation in a modelled installation starts with compressing the air by a compressor (C_{air}) and then cooling in the precooler (PC). Afterwards, cooled air is introduced into the first distillation column (RCI). The separation section of the installation consists of two columns. In column RCI oxygen is obtained, and the rest of the air is transported to the second column and is separated there into low-purity nitrogen (lN_2) and high-purity nitrogen (hN_2). A diagram of modelled cryogenic ASU is presented in Fig. 2.
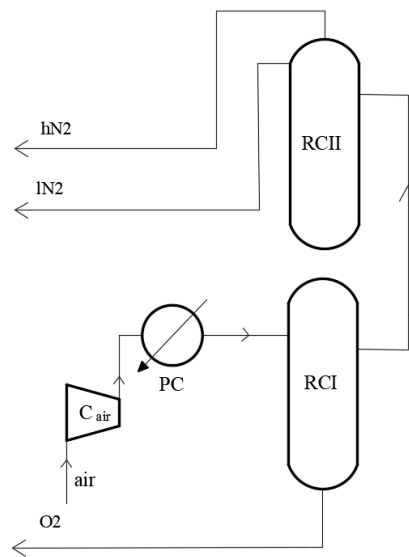

Figure 2: Diagram of modelled cryogenic unit.

3 Methodology

3.1 Cycle efficiency

The gross and net efficiencies of the power cycle have been calculated using the following formulae:

$$\eta_g = \frac{N_t}{\dot{Q}_{CC}} \,, \tag{1}$$

and

$$\eta_{\text{net}} = \frac{N_t - N_{CP}}{\dot{Q}_{CC}} \, , \tag{2}$$

where N_t is a combined power of turbines, $\dot{Q}_{CC}$ is a chemical energy rate of combustion, and N_{CP} is the power for the cycle own needs, and which can be expressed as

$$N_{CP} = N_{\text{ASU}} + N_{C_{\text{fuel}}} + N_{C_{O2}} + N_{P_{\text{H2O}}} + N_{P_{\text{SEC}}} + N_{C_{\text{CCS}}} \, , \tag{3}$$

where N_{ASU} is the power for oxygen production, $N_{C_{\text{fuel}}}$ is the power for fuel compressor, $N_{C_{O2}}$ is the power for oxygen compressor, $N_{P_{\text{H2O}}}$ is the power for water pump, $N_{P_{\text{SEC}}}$ is the power for SEC and $N_{C_{\text{CCS}}}$ is the power for CCS compressors needs.

Additionally, the cumulative cycle efficiency which is a product of the net efficiency of the power cycle and gasification process efficiency (η_{R_H}) has been calculated. The gasification process inside the gasifier was not calculated in this work but its efficiency has been taken from another paper regarding nCO2PP [21]. The cumulative efficiency is expressed as

$$\eta_{\text{cum}} = \eta_{R_H} \eta_{\text{net}} \, , \tag{4}$$

where the gasification process efficiency (η_{R_H}) according to the literature [26] is equal to 86.52% for the nCO2PP cycle.

3.2 Energy penalty and emissivity

For cryogenic oxygen production, an important parameter is the energy penalty of oxygen production:

$$e_{\text{pen}} = \frac{N_{\text{ASU}}}{3600 \dot{m}_{\text{O2}}} \, , \tag{5}$$

where N_{ASU} is the power for the needs of oxygen production and $\dot{m}_{\text{O2}}$ is the produced oxygen mass flow.

Due to the name of the cycle (negative CO_2 emission gas power plant), an essential factor is the emission potential of the whole system, which can be defined as [25–27]

$$e\text{CO}_2 = R \frac{\dot{m}_{4\text{CO}_2}}{N_t - N_{CP}} \, 3600 \, , \tag{6}$$

where $\dot{m}_{4CO2}$ is the mass flow rate of carbon dioxide at the outlet of the CCS, R is a factor describing the energy source as renewable energy (for sewage sludge is 90.0% according to Polish regulations [28]).

The emission calculations should be carried out properly and carefully if the power cycle is integrated with the carbon capture and storage unit. If an energy source is only partly considered a renewable source of energy, emissions should be multiplied by the factor that accounts for it. In this case, the relative emissions of carbon dioxide were multiplied by η_{net}. The relative emission is

$$\eta_{net} eCO_2 = \frac{N_t - N_{CP}}{\text{LHV}\dot{m}_{0fuel}} R \frac{\dot{m}_{4CO2}}{N_t - N_{CP}} 3600 = R \frac{\dot{m}_{4CO2}}{\dot{Q}_{CC}} 3600 , \qquad (7)$$

where LHV is the lower heating value.

The avoided eCO_2 for the negative emission power plant is a sum of emissions without CO_2 capture and the value of negative emissions obtained because of the application of renewable energy sources [27].

3.3 Ebsilon software

A numeric code for the purpose of the present analysis solves equations of mass and energy balance. According to the mass balance equation, the mass that flows into a channel is equal to the mass, which flows out of the channel [29, 30]. The mass balance is nothing else than the equation of continuity:

$$\sum_{i=1}^{n} \dot{m}_i = \sum_{j=1}^{m} \dot{m}_j , \qquad (8)$$

where $\dot{m}$ is a mass flow rate. According to the energy balance, the energy that flows into a device is equal to the energy, which outflows [29, 30] and can be written as

$$\sum_{i=1}^{n} \dot{m}_i \left(u_i + \frac{c_i}{2} + \frac{p_i}{\rho} + z_i g \right) + \dot{Q}_i = \sum_{j=1}^{m} \dot{m}_j \left(u_j + \frac{c_j}{2} + \frac{p_j}{\rho} + z_j g \right) + N_j , \quad (9)$$

where u is the internal energy, c is the velocity, p is the pressure, ρ is the density, z is the height, g is the gravitational acceleration, $\dot{Q}$ is the heat energy rate, and N is the mechanical power, and here $i = 1, 2, \ldots, n$, $j = 1, 2, \ldots, m$, and m and n represent streams that flow in the channel and flow out of the channel, respectively.

There are many various equations of state, which are used in industrial calculations [31]. The system under investigation was simulated using commercial plant engineering and thermodynamic process analysis software, Ebsilon Professional [32]. Ebsilon software uses the Peng-Robinson equation of state for real gas, instead of the Clapeyron ideal gas equation of state [29]. The software predefined models are clearly expressed by thermodynamic tables for steam. Appropriate choice of the thermodynamic models of real gases has crucial importance for the critical area [33, 34]. The crucial advantage of using the Peng-Robinson equation of state is obtaining a higher accuracy of calculation, especially near the gases and mixtures critical points. This fact is important for modelling real thermodynamic cycles. The Peng-Robinson equation takes into account intermolecular forces [34]. A disadvantage of this model is the fact that not all of the factors have been fully examined at the area of their critical point. On the other hand, the Clapeyron equation allows us to obtain results very fast but it idealizes all gases.

4   Calculation conditions

In the study, four analyses have been carried out. The first one is the nCO2PP connected with cryogenic ASU and with the exhaust bleed for sewage sludge gasification. The bleed is made between GT and GT$^{\mathrm{bap}}$, its pressure is 1.0 bar and temperature is 664.83°C, whereas the mass flow transported to the gasifier is 18.0 g/s. The second analysis is for the same cycle but without the bleed for gasification. Moreover, research on the cryogenic ASU model power consumption depending on the produced oxygen purity has been done. The fourth analysis refers to CO_2 purity at the end of the power cycle (point 5^{CCU} in Fig. 1). Traditionally it is assumed that the production of nitrogen oxides in gas turbines combustion chambers is connected with Zeldowicz's thermal mechanisms [35]. In order to properly model NO_x and CO_2 production in new devices, computational fluid dynamics (CFD) simulations are more convenient, because they allow us to take into account a distribution of components, production sources in particular chemical reactions, and velocity fields [36, 37]. The most important conditions for the ASU model are presented in Table 1.

Important assumptions of the nCO2PP cycle are stoichiometric combustion in oxygen as oxidizer and using sewage sludge as fuel. Fuel composition is as follows: 13.31% CO, 5.12% H_2, 11.46% CH_4, 59.29% CO_2, 8.03%

C_3H_8, and its lower heating value (LHV) is 17.44 MJ/kg. The rest of the assumptions and boundary conditions are presented in Table 2.

Table 1: Cryogenic ASU model condition.

Description	Symbol	Unit	Value
Air initial temperature	t^{0air}	$^\circ$C	15.0
Air initial pressure	p^{0air}	bar	1.0
Air compression pressure	p^{1air}	bar	5.8

Table 2: The nCO2PP model input data.

Parameter	Symbol	Unit	Value
Initial fuel temperature	t_{0fuel}	$^\circ$C	50.0
Initial oxygen temperature	t_{0O2}	$^\circ$C	40.0
Syngas fuel pressure before C_{fuel} compressor	p_{0fuel}	bar	1.0
Oxygen pressure before C_{O2} compressor	p_{0O2}	bar	1.0
Exhaust temperature after HE1, before SEC	t_5	$^\circ$C	65.42
CO_2 pressure after compressor C_{CCU}	p_{2CCU}	bar	40.0
CO_2 pressure after compressor C_{CCU}	p_{4CCU}	bar	90.0
H_2O temperature after HE4	t_{2-H_2O}	$^\circ$C	91.67
CO_2 temperature after HE3	t_{3-CCU}	$^\circ$C	110
Pressure after GT^{bap}	p_4	bar	0.078
Temperature after SEC	t_6	$^\circ$C	18.03
Turbine GT, internal efficiency (η_i)	η_{iGT}	–	0.89
Turbine GT^{bap}, η_i	$\eta_{iGT-bap}$	–	0.89
Fuel compressor C_{fuel}, η_i	$\eta_{iC-fuel}$	–	0.89
Oxygen compressor C_{O2}, η_i	η_{iC-O2}	–	0.87
Water pump P_{H2O}, η_i	η_{iP-H2O}	–	0.43
Water pump P_{SEC}, η_i	η_{iP-SEC}	–	0.80
CO_2 compressor C_{CO2-1}, η_i	$\eta_{iC-CO2-1}$	–	0.85
CO_2 compressor C_{CO2-2}, η_i	$\eta_{iC-CO2-2}$	–	0.85
Mechanical efficiency for all devices	η_m	–	0.99
Gasification process efficiency	η_{R_H}	–	0.8652
Temperature in the WCC	t_2	$^\circ$C	1100
Pressure in the WCC	p_2	bar	10.5
Exhaust mass flow after WCC	$\dot{m}_2$	g/s	100.0

5   Results

The following studies have been accomplished:

- analysis of the nCO2PP integrated with ASU which produces oxygen at 95.0% and 99.5% purity, and with the bleed for the gasification process;

- analysis of the nCO2PP integrated with ASU which produces oxygen at 95.0% and 99.5% purity, and without the bleed for the gasification process;

- analysis of power consumption of an individual cryogenic ASU model dependent on produced oxygen purity. In this case, constant oxygen mass flow was established as 21.7 g/s, and C_{air} compression to 5.8 bar;

- analysis of the impact of oxygen purity on the nCO2PP cycle efficiency;

- analysis of oxygen purity impact on the carbon dioxide purity at the end of the CCS installation.

In Table 3 the results for nCO2PP integrated with cryogenic ASU, with the bleed and without the bleed for the gasification process are presented. Two oxygen purities were taken into consideration, namely 95.0% and 99.5%. Figure 3 presents the obtained plot of the energy penalty of the cryogenic
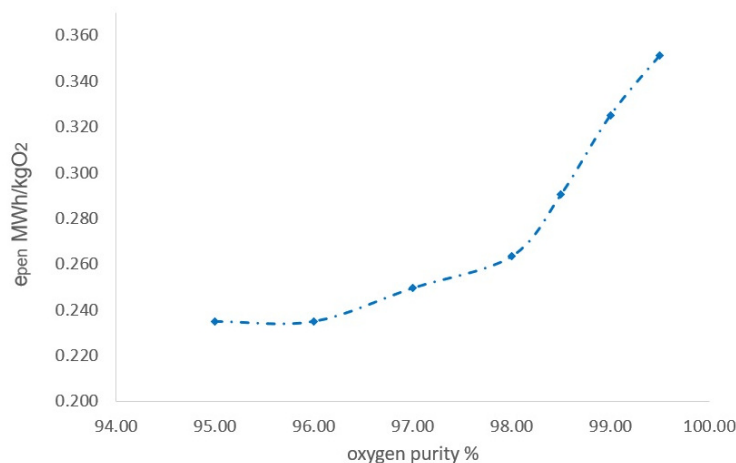

Figure 3: Results of power consumption of the modelled ASU dependent on produced oxygen purity.

Table 3: Results of the analyses of the nCO2PP integrated with the cryogenic ASU including the bleed for gasification process and excluding the bleed.

| Description | Symbol | Unit | Oxygen purity | | | |
| | | | 95.0% | | 99.5% | |
			nCO2PP + ASU + bleed	nCO2PP + ASU	nCO2PP + ASU + bleed	nCO2PP + ASU
Air mass flow	$\dot{m}_{0air}$	g/s	98.0	97.73	94.0	93.69
Oxygen mass flow	$\dot{m}_{0O2}$	g/s	22.64	22.48	21.7	21.55
ASU power consumption	N_{ASU}	kW	19.17	19.03	27.03	26.91
nCO2PP turbines output	N_t	kW	143.91	154.77	143.05	154.56
nCO2PP power for own needs	N_{CP}	kW	61.1	65.85	67.79	72.27
Chemical rate of combustion	$\dot{Q}_{CC}$	kW	306.08	303.88	306.27	304.80
nCO2PP gross efficiency	η_g	%	47.02	50.93	46.71	50.71
nCO2PP net efficiency	η_{net}	%	27.05	29.26	24.57	27.0
nCO2PP cumulative efficiency	η_{cum}	%	23.41	25.32	21.26	23.36
Emission of CO_2	eCO_2	kgCO_2/MWh	−782.54	-874.49	−860.98	−905.57
Relative emissivity of CO_2	$\eta_{net}eCO_2$	kgCO_2/MWh	−211.71	−255.89	−211.58	−244.49
Avoided emission of CO_2	Avoid eCO_2	kgCO_2/MWh	1652.03	1846.15	1817.63	1911.75
Energy penalty	e_{pen}	MWh/kgO_2	0.235	0.235	0.346	0.347

ASU dependent on the produced oxygen purity. It is important to mention that the considered ASU model is the same as the one which was integrated with the nCO2PP but independent and with constant oxygen mass flow. In Fig. 4 efficiencies characteristics of the whole cycles dependent on the generated oxygen purity are shown both for the cycle including bleed and excluding bleed. In the same figure, the results of the produced CO_2 purity for two power cycle cases are presented.
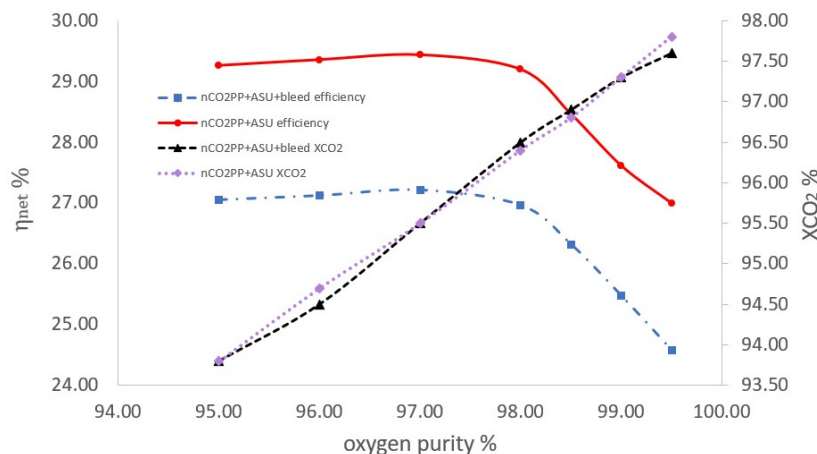
Figure 4: Results of the nCO2PP cycle efficiency and CO_2 purity in the exhaust dependent on produced oxygen purity.

6　　Discussion of the results

According to the results in Table 3, the cycle net efficiency is higher for combustion in the oxygen of 95.0% purity for both cases including and excluding the bleed. Although 99.5% is an extremely high value of oxygen purity and it is desirable in some industries like metallurgy, it is too high for the nCO2PP cooperating with cryogenic ASU. This high level of purity does not have a positive impact on cycle efficiency. Its advantage might be resulting in a smaller amount of nitrogen oxides in the exhaust [38, 39] but it was not considered in this work. With the enhancing oxygen purity, the temperature in the WCC should increase [40], but for the purpose of this analysis, the temperature in the WCC and exhaust mass flow were set and balanced at 1100°C and 100.0 g/s for every simulation. The analysis of the influence of oxygen purity on the nCO2PP efficiency showed (Fig. 4) that the most appropriate oxygen purity is 97.0%, because efficiency is growing until oxidizer purity reaches 97.0%. After surpassing this value, a rapid efficiency drop is observed. The most common statement is that oxygen at 95.0% purity is the most proper for the majority of the power cycles that work with oxy-fuel technology [41, 42].

Regarding the independent model of cryogenic ASU, it can be seen that the energy penalty does not change significantly until it reaches a purity of 96.0% (Fig. 3). After this value, it suddenly increases. It is supposed to

be a proper behaviour. In [42] Darde showed a similar characteristic, which was increasing after exceeding the value of 95.0% oxygen purity. In [13] also the power consumption dependent on ASU can be seen but the plot is more steady. It grows but significantly slower. The obtained energy penalty values are crucial factors for this ASU model and they are 0.235 MWh/kgO_2 for 95.0% purity, 0.263 MWh/kgO_2 for 98.0% purity, and 0.351 MWh/kgO_2 for 99.5% oxygen purity. The obtained values can be compared to the results from other works. Fu claims that the power consumption for 95.0% purity is 0.229 MWh/kgO_2 [9], Janusz-Szymańska states that for 97.0% oxygen purity, the power consumption is 0.247 MWh/kgO_2 [43], Aneke says about 0.357 MWh/kgO_2 for oxygen at purity 99.9% [14], and Tafone assumes 0.370 MWh/kgO_2 for 99.5% oxygen purity [44].

Results regarding the emissivity indicate that cycles with a combustion process with 99.5% oxygen achieved higher values of negative emission and avoided emission of CO_2 than the equivalent cycles with combustion in 95.0% oxygen.

There is one more point worth mentioning. According to the calculations, CO_2 purity is different for various oxygen purities. For the cycle case with the exhaust bleed, the CO_2 composition in the last point of the cycle (5^{CCU}) is 97.6% and 93.8% for 99.5% and 95.0% oxygen purity, respectively. For the cycle case excluding the bleed, CO_2 composition in mentioned point is 97.8% and 93.8% for 99.5% and 95.0% oxygen purity. A reasonable CO_2 purity for the oxy-combustion process is in the range of 95.0–97.0% [45,46]. In this work, this value is only achieved for 97.0% oxygen purity. Thus, as the authors [47] pointed out, in addition to electricity, the output product of the nCO2PP cycle is also carbon dioxide, and in such a context it makes as great sense as possible to raise its purity. CO_2 is a useful product and its purity for syngas from methane was examined in [47]. On the other hand, in [48] at the inlet of the carbon capture installation, the gas composition is as follows: 64.72% H_2O, 32.53% CO_2, 2.0% O_2, and 0.75% N_2. It means that in the model, the excess of oxygen and oxygen purity lower than 100.0% was assumed.

In this paper, oxy-fuel technology is considered in case of thermodynamic cycle with gas turbine. However, it would also be interesting to introduce oxy-combustion technology to piston engines. There were researches regarding piston engines with internal combustion and oxy-fuel before [49–51]. It would also be interesting to see how oxy-combustion technology can be introduced into piston engine with external combustion process e.g. Stirling engine like in [52].

7 Conclusions

In the paper, the impact of the cryogenic air separation unit on the negative CO_2 emission gas power plant was presented. As the results showed, the highest oxygen purity does not provide the most profitable cycle efficiency. Power consumption dependent on oxygen purity plot shows that attempts to obtain high purity oxygen may generate large power demand and due to that the cycle efficiency drop. However, it should be emphasized that increasing the purity of the oxygen injected into the combustion chamber has a beneficial effect on the purity of the captured carbon dioxide obtained from the CCU.

Acknowledgements

The research leading to these results has received funding from the Norway Grants 2014–2021 via the National Centre for Research and Development. This research has been prepared within the frame of the project: "Negative CO2 emission gas power plant" – NOR/POLNORCCS/NEGATIVE-CO2-PP/0009/2019-00 which is co-financed by the programme "Applied research" under the Norwegian Financial Mechanisms 2014–2021 POLNOR CCS 2019 – Development of CO2 capture solutions integrated in power and industry processes.

The part of work is a result of a project realized by Maja Kaszuba and it was financed by Radium Learning Through Research Programs.

Received 4 April 2023

References

[1] United States Environmental Protection Agency. https://www.epa.gov/ (accessed 20 March 2022).

[2] Our World in Data. https://ourworldindata.org (accessed 20 March 2022).

[3] Chen W., van der Ham L., Nijmeijer A., Winnubst L.: *Membrane-integrated oxy-fuel combustion of coal: Process design and simulation.* J. Membrane Sci. **492**(2015), 461–470.

[4] Merkel T., Lin H., Wei X., Baker R.: *Power plant post-combustion carbon dioxide capture: An opportunity for membranes.* J. Membrane Sci. **359**(2010), 126–139.

[5] Blamey J., Anthony E.J., Wang J., Fennell P.S.: *The calcium looping cycle for large-scale CO_2 capture.* Prog. Energ. Combust. Sci. **36**(2010), 260–279.

[6] Mikielewicz D., Wajs J., Ziółkowski P., Mikielewicz J.: *Utilisation of waste heat from the power plant by use of the ORC aided with bleed steam and extra source of heat.* Energy **97**(2016), 11–19.

[7] Ziółkowski P., Mikielewicz D., Mikielewicz J.: *Increase of power and efficiency of the 900 MW supercritical power plant through incorporation of the ORC.* Arch. Thermodyn. **34**(2013), 4, 51–71.

[8] Ye H., Zheng J., Li Y.: *Feasibility analysis and simulation of argon recovery in low oxygen-purity cryogenic air separation process with low energy consumption.* Cryogenics **97**(2019), 109–121.

[9] Fu C., Gundersen T.: *Using exergy analysis to reduce power consumption in air separation units for oxy-combustion processes.* Energy **44**(2012), 1, 60–68.

[10] Higginbotham P., White V., Fogash K., Guvelioglu G.: *Oxygen supply for oxycoal CO_2 capture.* Energy Proced. **4**(2011), 884−891.

[11] García-Luna S., Ortiz C., Carro A., Chacartegui R., Pérez-Maqueda L.A.: *Oxygen production routes assessment for oxy-fuel combustion.* Energy **254**(2022), B, 124303.

[12] Chorowski M., Gizicki W.: *Technical and economic aspects of oxygen separation for oxy-fuel purposes.* Arch. Thermodyn. **36**(2015), 1, 157–170.

[13] Fu Q., Kansha Y., Song C., Liu Y., Ishizuka M., Tsustumi A.: *A cryogenic air separation process based on self-heat recuperation for oxy-combustion plants.* Appl. Energ. **162**(2015), 1114–1121.

[14] Aneke M., Wang M.: *Potential for improving the energy efficiency of cryogenic air separation unit (ASU) using binary heat recovery cycles.* Appl. Therm. Eng. **81**(2015), 223–231.

[15] Kerry F.: *Industrial Gas Handbook: Gas Separation and Purification.* Taylor and Francis, New York 2006.

[16] Portillo E., Gallego Fernández L.M., Vega F., Alonso-Fariñas B., Navarrete B.: *Oxygen transport membrane unit applied to oxy-combustion coal power plants: A thermodynamic assessment.* J. Environ. Chem. Eng. **9**(2021), 4, 105266.

[17] Castillo R.: *Thermodynamic analysis of a hard coal oxyfuel power plant with high temperature three-end membrane for air separation.* Appl. Energ. **88**(2011), 5, 1480–1493.

[18] Gutiérrez F.A., García-Cuevas L.M., Sanz W.: *Comparison of cryogenic and membrane oxygen production implemented in the Graz cycle.* Energ. Convers. Manage. **271**(2022), 116325.

[19] Fu C., Gundersen T.: *Recuperative vapor recompression heat pumps in cryogenic air separation processes.* Energy **59**(2013), 708–718.

[20] Tesch S., Morosuk T., Tsatsaronis G.: *Comparative evaluation of cryogenic air separation units from the exergetic and economic points of view. Low-temperature Technologies.* IntechOpen, 2020. doi: 10.5772/intechopen.85765

[21] Yantovski E., Zvagolsky K.N., Gavrilenko V.A.: *The cooperate – demo power cycle.* Energ. Convers. Manage. **36**(1995), 6-9, 861–864.

[22] Yantovski E.: *Zero emission fuel-fired power plants concept.* Energ. Convers. Manage. **37**(1996), 6-8, 867–877.

[23] Sanz W., Hustad C.-W., Jericha H.: *First generation Graz cycle power plant for near-term development.* In: Proc.. ASME Turbo Expo 2011, 969–979.

[24] Gou C., Cai R., Hong H.: *A novel hybrid oxy-fuel power cycle utilizing solar thermal energy.* Energy **32**(2007), 9, 1707–1714.

[25] Ziółkowski P., Madejski P., Amiri M., Kuś T., Stasiak K., Subramanian N., Pawlak-Kruczek H., Badur J., Niedźwiedzki Ł., Mikielewicz D.: *Thermodynamic analysis of negative CO2 emission power plant using Aspen Plus, Aspen Hysys, and Ebsilon software.* Energies **14**(2021), 19, 6304.

[26] Ziółkowski P., Stasiak K, Amiri M., Mikielewicz D.: *Negative carbon dioxide gas power plant integrated with gasification of sewage sludge.* Energy **262**(2023), B, 125496.

[27] Madejski P., Chmiel K., Subramanian N., Kuś T.: *Methods and techniques for CO_2 capture: Review of potential solutions and applications in modern energy technologies.* Energies **15**(2022), 3, 887.

[28] Regulation of the Minister of Environment of 8 June 2016 on the technical conditions for the qualification of part of the energy recovered from thermal transformation of waste). J. Laws Republic of Poland (in Polish).

[29] Badur J.: *Five Lectures in Modern Fluid Thermomechanics.* Wydawn. IMP PAN, Gdańsk 2005 (in Polish).

[30] Kaszuba M., Ziółkowski P., Mikielewicz D.: *Thermodynamical analysis of integration of a negative emission power plant cycle with oxygen generation station.* In: Proc. 7th Conf. on Contemporary Problems of Thermal Engineering, CPOTE 2022. Silesian UT, Warszawa 2022, 619–630.

[31] Ibrahim M., Skaugen G., Ertesvåg I.S.: *An extended corresponding states equation of state (EoS) for CCS industry.* Chem. Eng. Sci. **137**(2015), 572–582.

[32] Ebsilon® Professional 15.00, Steag Energy Services GmbH, Flextek 2022.

[33] Mikielewicz J., Bieliński H., Mikielewicz D.: *Outline of Thermodynamics* Wydawn. IMP PAN, Gdańsk 1996 (in Polish).

[34] Peng D.-Y., Robinson D.: *A new two-constant equation of state.* Ind. Eng. Chem. Fundam. **15**(1976), 1, 59–64.

[35] Jesionek K., Chrzczonowski A., Ziółkowski P, Badur J.: *Power enhancement of the Brayton cycle by steam utilization.* Arch. Thermodyn. **33**(2012), 3, 39–50.

[36] Badur J., Stajnke M., Ziółkowski P., Jóźwik P., Bojar Z., Ziółkowski P.J.: *Mathematical modeling of hydrogen production performance in thermocatalytic reactor based on the intermetallic phase of Ni_3Al.* Arch. Thermodyn. **40**(2019), 3, 3–26.

[37] Ziółkowski P.: *Porous structures in aspects of transpirating cooling of oxycombustion chamber walls.* In: AIP Conf. Proc. AIoP **2077**(2019), 020065 .

[38] Normann F., Andersson K., Leckner B., Johnsson F.: *Emission control of nitrogen oxides in the oxy-fuel process.* Prog. Energ. Combust. Sci. **35**(2009), 5, 385–397.

[39] Ziółkowski P., Zakrzewski W., Kaczmarczyk O., Badur J.: *Thermodynamic analysis of the double Brayton cycle with the use of oxy combustion and capture of CO_2.* Arch. Thermodyn. **34**(2013), 2, 23–38.

[40] Koohestanian E., Shahraki F.: *Review on principles, recent progress, and future challenges for oxy-fuel combustion CO_2 capture using compression and purification unit.* J. Environ. Chem. Eng. **9**(2021), 4, 105777.

[41] Banaszkiewicz T., Chorowski M., Gizicki W.: *Comparative analysis of oxygen production for oxy-combustion application.* Energy Proced. **51**(2013), 127–134.

[42] Darde A., Prabhakar R., Tranier J.-P., Perrin N.: *Air separation and fuel gas compression and purification units for oxy-coal combustion systems.* Energy Proced. **1**(2009), 527–534.

[43] Janusz-Szymańska K., Dryjańska A.: *Possibilities for improving the thermodynamic and economic characteristics of an oxy-type power plant with a cryogenic air separation unit.* Energy **85**(2015), 45–61.

[44] Tafone A., Dal Magro F., Romagnoli A.: *Integrating an oxygen enriched waste to energy plant with cryogenic engines and air separation unit: Technical, economic and environmental analysis.* Appl. Energ. **231**(2018), 423–432.

[45] Goto K., Kazama S., Furukawa A., Serizawa M., Aramaki S., Shoji K.: *Effect of CO_2 purity on energy requirement of CO2 capture process.* Energy Proced. **37**(2013), 806–812.

[46] Murugan A., Brown R.J.C, Wilmot R., Hussain D., Bartlett S., Brewer P.J., Worton D.R., Bacquart T., Gardiner T., Robinson R.A., Finlayson A.: *Performing quality assurance of carbon dioxide for carbon capture and storage.* J. Carbon Res. **6**(2020), 4, 76.

[47] Ertesvåg I.E., Madejski P., Ziółkowski P., Mikielewicz D.: *Exergy analysis of a negative CO_2 emission gas power plant based on water oxy-combustion of syngas from sewage sludge gasification and CCS.* Energy **278**(2023), 127690.

[48] Kotowicz J., Job M.: *Thermodynamic and economic analysis of a gas turbine combined cycle plant with oxy-combustion.* Arch. Thermodyn. **34**(2013), 4, 215–233.

[49] Serrano J.R., Arnau F.J., García-Cuevas L.M., Gutiérrez F.A.: *Coupling an oxygen generation cycle with an oxy-fuel combustion spark ignition engine for zero NOx emissions and carbon capture: A feasibility study.* Energ. Convers. Manage. **284**(2023), 116973.

[50] Wu Z., Yu X., Fu L., Deng J., Hu Z., Li L.: *A high efficiency oxyfuel internal combustion engine cycle with water direct injection for waste heat recovery.* Energy **70**(2014), 110–120.

[51] Peng J., Li X.: *Oxyfuel combustion in IC engines. Internal Combustion Engines – Recent Advances.* IntechOpen, 2022. doi: 10.5772/intechopen.107155

[52] Kropiwnicki J.: *Analysis of start energy of Stirling engine type alpha.* Arch. Thermodyn. **40**(2019), 3, 243–259.